J|A|C|S
ARTICLES
Published on Web 05/08/2002

Hydroxyl Radical Reactivity with Nitrobenzene in Subcritical and Supercritical Water

Junbo Feng, Sudhir N. V. K. Aki, John E. Chateauneuf,*,† and Joan F. Brennecke*

Contribution from the Department of Chemical Engineering, University of Notre Dame, Notre Dame, Indiana 46556

Received April 30, 2001. Revised Manuscript Received December 31, 2001

Abstract: The bimolecular rate constants of the addition reaction between hydroxyl radical (•OH) and nitrobenzene ($C_6H_5NO_2$) were measured in subcritical and supercritical water (SCW) at temperatures between ambient and 390 °C. The measured bimolecular rate constants showed distinctly non-Arrhenius behavior (i.e., essentially no increase with temperature) from ambient to 350 °C, but increased in the slightly subcritical and supercritical region between 350 and 390 °C. These data were modeled reasonably well over the entire temperature range with a three-step reaction mechanism, originally proposed by Ashton et al.[1] This model includes the formation of a π-complex intermediate as the precursor of the nitrohydroxycyclohexadienyl radical.

Introduction

Supercritical water oxidation (SCWO) has drawn substantial interest since it is an efficient and environmentally benign technology for the complete destruction of organic compounds in aqueous waste streams.[2] Typically the oxidation process will occur at conditions above the critical point of water ($P_C = 218$ atm, $T_C = 374$ °C), where organic compounds, gases, and water can form single phase mixtures. Single-phase operation can eliminate mass transfer limitations, with the added benefit of high intrinsic reaction rates provided by the relatively high temperature.

Detailed kinetic models of the SCWO process, in terms of elementary reaction steps, describe the basic chemistry and, thus, may have some predictive value. Indeed, detailed chemical kinetic models[3−17] have had some success in reproducing experimental data. The biggest concern is whether the rate constants for each elementary reaction, taken from the combustion literature (gas-phase measurements) with some solvent corrections, really reflect the actual reaction rate constants under supercritical water (SCW) conditions. Verification of the values of the individual rate constants important in modeling SCWO has been very limited.[13,15] Measurement of these individual rate constants in SCW could dramatically improve the confidence in modeling SCWO processes with elementary kinetics. In this study we attempt to make the first step toward such measurements.

The goal of the present work is to study hydroxyl radical, •OH, reactivity since it has been shown to be one of the primary oxidizing species during SCWO.[2,8,14,16] Another important oxidant is $^{\bullet}HO_2$.[15,17] We have chosen the addition of •OH to nitrobenzene, $C_6H_5NO_2$, to form the nitrohydroxycyclohexadienyl radical ($^{\bullet}OHC_6H_5NO_2$) as a model reaction to study •OH reactivity, as shown in eq 1.

$$C_6H_5NO_2 + {}^{\bullet}OH \xrightarrow{k_{bi}} {}^{\bullet}OHC_6H_5NO_2 \qquad (1)$$

Hydrogen abstraction by hydroxyl radical comprises a particularly important class of reactions in SCWO processes[16,18−20] and these types of reactions can also be studied. Since direct measurement of hydroxyl radical concentration is difficult and the radicals formed by hydrogen abstraction from many

* Corresponding author. Fax: (574) 631−8366. E-mail: jfb@nd.edu.
† Current address: Department of Chemistry, Western Michigan University, Kalamazoo, MI 49008. Fax: (616) 387-2909. E-mail: chateauneuf@wmich.edu.

(1) Ashton, L.; Buxton, G. V.; Stuart, C. R. *J. Chem. Soc., Faraday Trans.* **1995**, *91*, 1631−1633.
(2) Savage, P. E. *Chem. Rev.* **1999**, *99*, 603−621.
(3) Holgate, H. R.; Tester, J. W. *Combust. Sci. Technol.* **1993**, *88*, 369−397.
(4) Holgate, H. R.; Tester, J. W. *J. Phys. Chem.* **1994**, *98*, 810−822.
(5) Webley, P. A.; Tester, J. W. *Energy Fuels* **1991**, *5*, 411−419.
(6) Gopalan, S.; Savage, P. E. *AIChE J.* **1995**, *41*, 1864−1873.
(7) Savage, P. E.; Yu, J. L.; Stylski, N.; Brock, E. E. *J. Supercrit. Fluids* **1998**, *12*, 141−153.
(8) Savage, P. E.; Rovira, J.; Stylski, N.; Martino, C. J. *J. Supercrit. Fluids* **2000**, *17*, 155−170.
(9) Gopalan, S.; Savage, P. E. In *Innovations in Supercritical Fluids−Science and Technology*; Hutchenson, K. W., Foster, N. R., Eds.; ACS Symp. Ser. No. 608; American Chemical Society: Washington, DC, 1995; pp 217−231.
(10) Dagaut, P.; Demarcillac, B. D.; Tan, Y.; Cathonnet, M.; Boettner, J. C. *J. Chim. Phys.-Chim. Biol.* **1995**, *92*, 1124−1141.
(11) Dagaut, P.; Cathonnet, M.; Boettner, J. C. *J. Supercrit. Fluids* **1996**, *9*, 33−42.
(12) Brock, E. E.; Savage, P. E. *AIChE J.* **1995**, *41*, 1874−1888.
(13) Croiset, E.; Rice, S. F.; Hanush, R. G. *AIChE J.* **1997**, *43*, 2343−2352.
(14) Tester, J. W.; Holgate, H. R.; Armellini, F. J.; Webley, P. A.; Killilea, W. R.; Hong, G. T.; Barner, H. E. In *Emerging Technologies in Hazardous Waste Management III*; Tedder, D. W., Pohland, F. G., Eds.; ACS Symp. Ser. No. 518; American Chemical Society: Washington, DC, 1993; pp 35−76.
(15) Maharrey, S. P.; Miller, D. R. *J. Phys. Chem. A* **2001**, *105*, 5860−5867.
(16) Brock, E. E.; Savage, P. E.; Barker, J. R. *Chem. Eng. Sci.* **1998**, *53*, 857−867.
(17) DiNaro, J. L.; Howard, J. B.; Green, W. H.; Tester, J. W.; Bozzelli, J. W. *J. Phys. Chem. A* **2000**, *104*, 10576−10586.
(18) Brock, E. E.; Oshima, Y.; Savage, P. E.; Barker, J. R. *J. Phys. Chem.* **1996**, *100*, 15834−15842.
(19) Rice, S. F.; Hunter, T. B.; Ryden, A. C.; Hanush, R. G. *Ind. Eng. Chem. Res.* **1996**, *35*, 2161−2171.
(20) Rice, S. F.; Croiset, E. *Ind. Eng. Chem. Res.* **2001**, *40*, 86−93.

10.1021/ja0110980 CCC: $22.00

compounds of interest in SCWO are difficult to detect, an attractive method to monitor hydrogen abstraction reactions involves the use of competitive kinetics, where a hydroxyl radical addition reaction is the probe. Thus, we view the hydroxyl radical addition reaction investigated here as a first step in the investigation of other individual reaction rates that are of particular interest to SCWO. In general, it is not possible to measure rates of individual reactions of •OH occurring during a SCWO process itself because multiple reactions occur simultaneously and the concentration of •OH is quite low. We circumvent these difficulties by using pulse radiolysis to generate high concentrations of •OH. Pulse radiolysis is a particularly attractive method for investigating SCW processes, since it allows the generation of •OH without the use of reactive additives.

Pulse radiolysis has been used recently for a variety of studies in supercritical fluids,[21−25] including work in SCW.[19−21,23] Hart and co-workers,[27] and more recently Wu and co-workers,[26] have observed the solvated electron in supercritical water. In work closely related to the present study, Ferry and Fox[22,23] used pulse radiolysis to study the *decay* kinetics of the hydroxycyclohexadienyl radical formed from the addition of •OH to benzene and anions of pentabromophenol, pentachlorophenol, and pentafluorophenol in SCW. The reactivity of carbonate radical with amino compounds was also studied in SCW using pulse radiolysis.[23] However, to our knowledge, this is the first report of the bimolecular rate constants for a reaction involving the addition of •OH in SCW. In this study, the rate of the reaction of •OH with nitrobenzene was determined by studying the growth kinetics of the intermediate product that leads to the formation of the nitrohydroxycyclohexadienyl radical.

The rate constant for the addition of •OH to nitrobenzene in water at ambient conditions is $3.2 \pm 0.4 \times 10^9$ M^{-1} s^{-1},[28] which is very close to the diffusion-controlled limit. The influence of supercritical fluids (SCFs) on reactions that would normally occur at the diffusion-controlled limit in liquids or gases has been of particular interest.[29] Much of the recent work[30−32] points to the conclusion that reactions that would normally occur at the diffusion-controlled limit in liquids also occur at the normal diffusion-controlled limit in SCFs, in contrast to some early speculations. In particular, we have shown that the triplet−triplet annihilation of anthracene remains diffusion controlled even at SCW conditions.[32] Therefore, one of the objectives of the current study might be to determine if the addition of •OH to $C_6H_5NO_2$ is diffusion controlled in SCW. However, Ashton et al.[1] studied the addition of •OH to $C_6H_5NO_2$ in water at temperatures from ambient to 200 °C and found that the rate constant did not follow Arrhenius behavior and was well below the diffusion-controlled limit. They proposed a three-step mechanism, involving the formation of a π-intermediate complex, that provided a good representation of the non-Arrhenius behavior at temperatures from ambient to 200 °C.

Here we extend the work of Ashton et al.[1] to include rate constants in water for the addition of •OH to $C_6H_5NO_2$ at temperatures to 390 °C. Although we find that the reaction rate measurably increases at the highest temperatures, the three-step mechanism proposed by Ashton et al.[1] is able to provide a good model of the rate constants over the entire temperature range from ambient to supercritical conditions.

Experimental Section

Materials. Nitrobenzene (Sigma-Aldrich, 99+%) was used as received. Water was filtered to 16 MΩ using a Millipore Reagent Water System at Notre Dame Radiation Laboratory. All solutions were saturated with N_2O (Mittler, 99.0%, minimum) before irradiation.

Pulse Radiolysis Apparatus. The pulse radiolysis experiments were conducted using the Notre Dame Radiation Laboratory Titan Beta Model TBS-8/16-1S electron linear accelerator. This system provides a pulse (1−15 ns) of 8 MeV electrons. The details of this pulse radiolysis system using time-resolved absorption detection are described elsewhere.[33,34] One modification of the system to accommodate the high-pressure, high-temperature optical cell is that we are unable to perform dosimetry on the system. However, we do monitor the dose entering the cell to ascertain stable operation. A 1000 W xenon lamp was used to monitor the transient absorption. The data acquisition system includes a Spex 270M monochromator and a Lecroy 7200A digital storage oscilloscope with a 7242B plug-in module. A Gateway 2000 4DX2-66V computer was used for experimental control.

Experiments were performed with continuous flow of the single phase aqueous solution to prevent the buildup of unwanted byproducts. The high-pressure, high-temperature flow system is shown in Figure 1. The main features of this system include a high-pressure, high-temperature optical cell, an Eldex model AA-100-S metering pump, and a Tescom model 26-1723-24 back-pressure regulator. The details of the high-pressure, high-temperature cell have been given elsewhere.[32] In this study, one of the sapphire windows has been replaced with a honeycomb radiolysis "window" made of Inconel 718.[35] This metal window was thick enough to withstand high pressure and temperature but thin enough to allow the passage of high-energy electrons from the accelerator.

An Eldex metering pump was used to pump the N_2O saturated feed solution to the cell at the required flow rate, which was typically on the order of 1 to 5 cm^3 min^{-1}, depending on the temperature, to provide a residence time of 1 ± 0.3 min in the cell. Three meters of coiled SS-316 tubing (0.635 cm o.d. by 0.386 i.d.) was used to dampen the pressure fluctuations generated by the pump, which were typically on the order of ±2.5 bar. The feed was preheated to the same temperature as the optical cell with a Thermolyne heating tape that was controlled with an Omega model CS-6001-K temperature controller, and the temperature was measured with a K-type thermocouple (Omega Model KMTIN-062U-6). The optical cell was heated using four 150 W Watlow Firerod cartridge heaters that were controlled with an Omega model MCS 6081-K temperature controller to ±2 °C. The temperature of the cell was measured to ±1 °C by direct contact of a type K thermocouple (Omega Model KTIN-116G-12) with the fluid in the cell. The cell was well insulated with Zircar type ECO-1200A silica alumina insulation.

(21) Zhang, J.; Connery, K. A.; Brennecke, J. F.; Chateauneuf, J. E. *J. Phys. Chem.* **1996**, *100*, 12394−12402.
(22) Ferry, J. L.; Fox, M. A. *J. Phys. Chem. A* **1998**, *102*, 3705−3710.
(23) Ferry, J. L.; Fox, M. A. *J. Phys. Chem. A* **1999**, *103*, 3438−3441.
(24) Takahashi, K.; Cline, J. A.; Bartels, D. M.; Jonah, C. D. *Rev. Sci. Instrum.* **2000**, *71*, 3345−3350.
(25) Dimitrijevic, N. M.; Takahashi, K.; Bartels, D. M.; Jonah, C. D.; Trifunac, A. D. *J. Phys. Chem. A* **2000**, *104*, 568−576.
(26) Wu, G.; Katsumura, Y.; Muroya, Y.; Li, X.; Terada, Y. *Chem. Phys. Lett.* **2000**, *325*, 531−536.
(27) Michael, B. D.; Hart, E. J.; Schmidt, K. H. *J. Phys. Chem.* **1971**, *75*, 2798−2805.
(28) Neta, P.; Dorfman, L. M. *Adv. Chem. Ser.* **1968**, *81*, 210−221.
(29) Brennecke, J. F.; Chateauneuf, J. E. *Chem. Rev.* **1999**, *99*, 433−452.
(30) Roberts, C. B.; Zhang, J.; Chateauneuf, J. E.; Brennecke, J. F. *J. Am. Chem. Soc.* **1993**, *115*, 9576−9582.
(31) Zhang, J.; Roek, D. P.; Chateauneuf, J. E.; Brennecke, J. F. *J. Am. Chem. Soc.* **1997**, *119*, 9980−9991.
(32) Kremer, M. J.; Connery, K. A.; DiPippo, M. M.; Feng, J.; Chateauneuf, J. E.; Brennecke, J. F. *J. Phys. Chem. A* **1999**, *103*, 6591−6598.
(33) Janata, E.; Schuler, R. H. *J. Phys. Chem.* **1982**, *86*, 2078−2084.
(34) Hug, G. L.; Wang, Y. C.; Schoneich, C.; Jiang, P. Y.; Fessenden, R. W. *Radiat. Phys. Chem.* **1999**, *54*, 559−566.
(35) Zhang, J.; Connery, K. A.; Strebinger, R. B.; Brennecke, J. F.; Chateauneuf, J. E. *Rev. Sci. Instrum.* **1995**, *66*, 3555−3559.

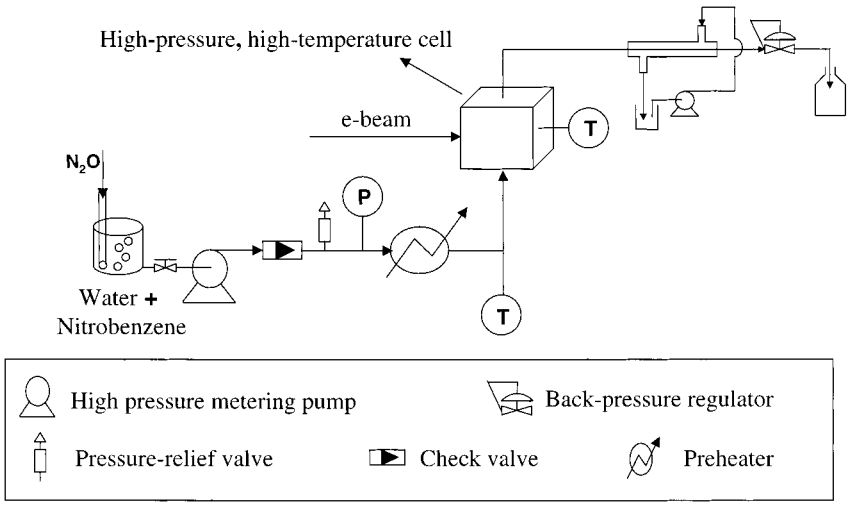

Figure 1. Schematic of the pulse radiolysis apparatus and the high-pressure, high-temperature flow system.

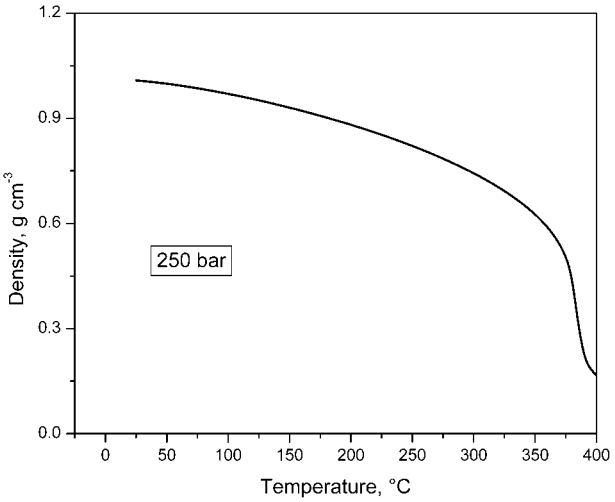

Figure 2. Density of water as a function of temperature at 250 bar.[36]

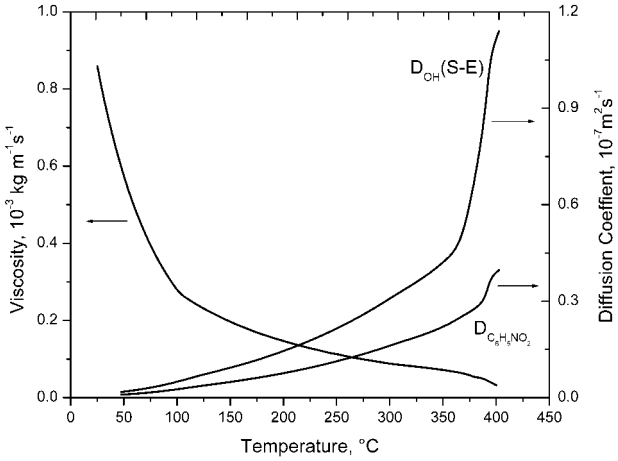

Figure 3. Viscosity of water and estimated diffusion coefficients of nitrobenzene as well as hydroxyl radical as a function of temperature at 250 bar. The diffusion coefficient of nitrobenzene is estimated with the Wilke−Chang equation (see text) and the diffusion coefficient of hydroxyl radical is estimated with the Stokes−Einstein equation (see text).

A Tescom back-pressure regulator was used to maintain the pressure at the desired value to ±2.5 bar. A Heise pressure transducer, model 901A, was used to monitor the system pressure to ±0.24 bar. A single-pass heat exchanger was used to cool the solution. A High-Pressure Equipment safety valve, model 15-61AF1, was used to ensure the safe operation of the flow system. All tubing and fittings were from High-Pressure Equipment and were rated to 1000 bar.

All the experimental data were obtained at a pressure of 250 bar in order to ensure single-phase operation. This pressure is above the vapor pressure of water at subcritical temperatures so those experiments involved single phase compressed liquids. Of course, above the critical temperature, the system is a single phase supercritical fluid. The density of pure water as a function of temperature at 250 bar is shown in Figure 2.[36] The density drops slowly except within about 25 °C of the critical temperature (374 °C). At the highest temperature studied (390 °C) the density has dropped to about 0.2 g cm^{-3}. The large decrease in viscosity with increasing temperature,[36] along with the concomitant increase in solute diffusion coefficients, is shown in Figure 3. The highest concentration of nitrobenzene used was 14 mM at ambient conditions, so we do not expect its presence to significantly change the physical properties from that of pure water. Nitrobenzene is soluble in water at these low concentrations at both ambient and supercritical conditions.

Production of •OH Radical. Pulse radiolysis involves the injection of high-energy electrons from an accelerator into the sample. Water absorbs energy from the ionizing radiation, leading to the formation of both stable species and reactive intermediates.[37] Typical species formed upon radiolysis of water are shown in eq 2.

$$H_2O \rightarrow H_2, H_2O_2, H^\bullet, {}^\bullet OH, e_{aq}^-, \ldots \quad (2)$$

The principal reactive intermediates are the hydroxyl radical, which exhibits oxidizing properties, and the hydrated electron, which exhibits reducing properties. Although there are differences in the radiolysis of liquid (products shown above) and gaseous samples,[37] we anticipate that the radiolysis of SCW will more closely resemble that occurring in the liquid phase because, even at the supercritical temperatures we studied, the density is quite liquidlike (see Figure 2). Since we are solely interested in studying the reactivity of •OH, the potential interference from the solvated electron (e^-_{aq}) was eliminated in the traditional fashion, i.e., by the addition of a scavenger, N_2O:[33]

$$e_{aq}^- + N_2O \rightarrow N_2 + O^{\bullet -} \quad (3)$$

$$O^{\bullet -} + H_2O \rightarrow OH^\bullet + OH^- \quad (4)$$

This leads to the formation of additional hydroxyl radicals and creates

(36) Hill, P. G. *J. Phys. Chem. Ref. Data* **1990**, *19*, 1233−1274.

(37) Matheson, M. S.; Dorfman, L. M. *Pulse Radiolysis*; M.I.T. Press: Cambridge, MA, 1969.

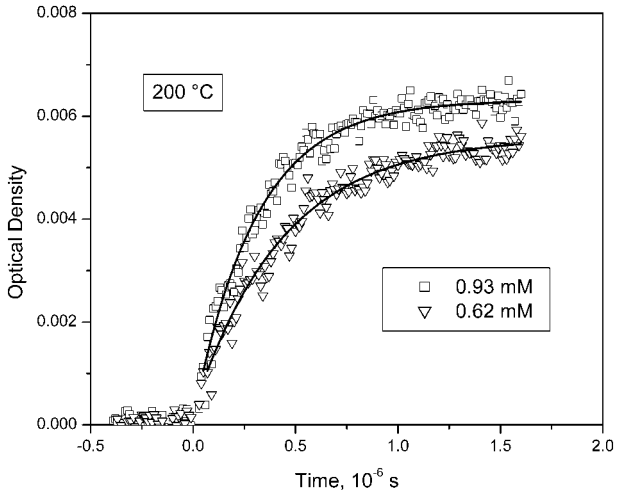

Figure 4. Typical growth profiles at 405 nm of nitrohydroxycyclohexadienyl radical, $^{\bullet}OHC_6H_5NO_2$, at two different nitrobenzene concentrations at 200 °C and 250 bar; the solid lines indicate the best fits of the exponential growths.

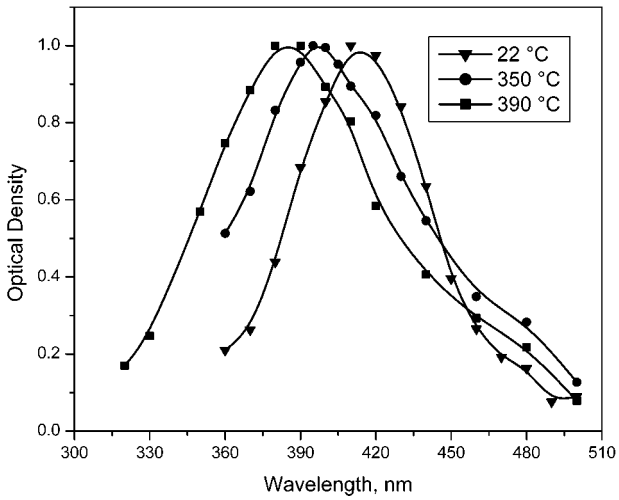

Figure 5. Transient absorption spectra of nitrohydroxycyclohexadienyl radical, $^{\bullet}OHC_6H_5NO_2$, at 250 bar and T = 22, 350, and 390 °C.

very nearly a one-radical system consisting of $^{\bullet}OH$ in subcritical or supercritical water. However, observation of hydroxyl radical concentration is difficult due to its ultraviolet absorption and low extinction coefficient. Therefore, we monitor the increase in concentration of the reaction product, nitrohydroxycyclohexadienyl radical ($^{\bullet}OHC_6H_5NO_2$), rather than the decrease in concentration of the hydroxyl radical. Hydroxyl radical is formed within the pulse width of the high-energy electrons (less than 15 ns), whereas the nitrohydroxycyclohexadienyl radical product forms, dependent upon nitrobenzene concentration and reaction conditions, over a time scale of 500 ns to 2 μs.

Analysis of Growth Kinetics. The rate of the formation of $^{\bullet}OHC_6H_5NO_2$ from the addition of hydroxyl radical to nitrobenzene is given by eq 5:

$$\text{rate} = \frac{\mathrm{d}[^{\bullet}OHC_6H_5NO_2]}{\mathrm{d}t} = k_{bi}[C_6H_5NO_2][^{\bullet}OH] \qquad (5)$$

In this study the concentration of $C_6H_5NO_2$ was much greater than the concentration of $^{\bullet}OH$ so the reaction could be analyzed with pseudo-first-order kinetics. The concentration range of $C_6H_5NO_2$ was 1−5 mM at reaction conditions, whereas that of $^{\bullet}OH$ is in the μM range.

The rate of disappearance of $^{\bullet}OH$ (eq 7) is the sum of the intrinsic solvent decay (eq 6) and the negative of the rate of reaction to form $^{\bullet}OHC_6H_5NO_2$ (eq 5).

$$^{\bullet}OH \xrightarrow{k'} \text{solvent decay} \qquad (6)$$

$$-\frac{\mathrm{d}[^{\bullet}OH]}{\mathrm{d}t} = k'[^{\bullet}OH] + k_{bi}[C_6H_5NO_2][^{\bullet}OH] \qquad (7)$$

Since the nitrobenzene concentration, $[C_6H_5NO_2]$, is in huge excess, the change in the concentration of $C_6H_5NO_2$ is negligible and hence

$$k_{obs} = k' + k_{bi}[C_6H_5OH] \qquad (8)$$

Using the growth in the absorbance of the product, $^{\bullet}OHC_6H_5NO_2$, as a function of time, we are able to obtain the pseudo-first-order observed rate constants at each temperature and pressure using standard kinetic analysis.[38] Specifically, analysis of absorbance versus time traces was carried out using ORIGIN software (Version 6, Microcal Software Inc.,) to fit the growth kinetics. Two typical growth profiles are shown in Figure 4 at two different nitrobenzene concentrations. The solid line shows the computer fit for the growth kinetics. The 95% confidence intervals on the growth rate constants were typically less than ±10%. As expected, the absorption of $^{\bullet}OHC_6H_5NO_2$ reaches the maximum (equilibrium) value faster at the higher nitrobenzene concentration.

Especially at higher temperatures, the decay of the concentration of the reaction product, $^{\bullet}OHC_6H_5NO_2$, is apparent. Since it was not our purpose to measure the kinetics of the nitrohydroxycyclohexadienyl radical decay, which could be first order, second order, or even mixed order, we do not present any results for its disappearance here. As shown previously[39] in such cases, a reliable method to obtain the growth kinetics is fitting just the growth at a time scale where the growth and subsequent plateau is present but no decay is apparent. This is the procedure used in this study. In most cases the two longest time scales that did not show decay (e.g., 500 ns and 1 μs) gave consistent (±10−15%) values of the growth rate constant.

The bimolecular rate constant, k_{bi}, for this addition reaction at each state point was obtained from a linear plot of k_{obs} as a function of nitrobenzene concentration, as suggested by eq 8.

Results

Below we describe the kinetics of the formation of nitrohydroxycyclohexadienyl radical from the reaction of hydroxyl radical with nitrobenzene. First, we will present the absorption spectrum of the nitrohydroxycyclohexadienyl radical and show how it shifts with temperature. Then, we will show the bimolecular rate constants obtained for the reaction of nitrobenzene with hydroxyl radical in water at temperatures from ambient to 390 °C.

Absorption Spectrum of Nitrohydroxycyclohexadienyl Radical ($^{\bullet}OHC_6H_5NO_2$). We found that the nitrohydroxycyclohexadienyl radical intermediate ($^{\bullet}OHC_6H_5NO_2$) absorbs strongly at 410 nm at ambient conditions, in agreement with literature data.[28] The absorption spectrum of $^{\bullet}OHC_6H_5NO_2$ was measured at temperatures between ambient and 390 °C and typical normalized absorption spectra at three temperatures are shown in Figure 5. At higher temperatures the signal-to-noise ratio was low due to the decreased solution density. Therefore, the number of shots averaged to determine each data point was increased from about 10 at ambient conditions to 60−100 at the higher temperatures.

(38) Capellos, C.; Bielski, B. H. J. *Mathematical Description of Chemical Kinetics in Solution*; Wiley-Interscience: New York, 1972.

(39) Scaiano, J. C.; Stewart, L. C. *J. Am. Chem. Soc.* **1983**, *105*, 3609−3614.

The absorption maximum shifted to shorter wavelengths (a blue shift) with increasing temperature. At supercritical conditions, the absorption maximum had shifted approximately 20 nm, to 390 nm. At all temperatures the growth of $^{\bullet}OHC_6H_5NO_2$ was measured at the absorption maximum and these profiles were used to calculate the observed rate constants. The blue solvatochromic shift of the $\pi \rightarrow \pi^*$ absorbance of $^{\bullet}OHC_6H_5NO_2$ indicates that the excited state is more polar than the ground state. Reduced solution density and reduced hydrogen bonding at higher temperatures results in less stabilization of the excited state, and a shift in the absorption maximum to higher energies. Similar behavior has been observed previously for benzophenone in subcritical and supercritical water.[40]

It should be noted that the stability of nitrobenzene in subcritical and supercritical water was tested prior to irradiation and any studies of the formation of nitrohydroxycyclohexadienyl radical. This was accomplished by flowing nitrobenzene solution through the reactor system and analyzing the effluent by gas chromatography. Although hydrolysis is certainly a possibility, the decrease in the nitrobenzene concentration was less than (10 ± 5)% at all conditions studied. Thus, the rates of hydrolysis and thermal decomposition are sufficiently slow at temperatures below 390 °C that nitrobenzene can be considered stable for the short times (on the order of 1−2 min) that the solution is at elevated temperatures. This is in agreement with a previous report that indicates less than 5% conversion of nitrobenzene in water at 440 °C when the residence times are less than 3 min and there is no oxygen present.[41]

Bimolecular Rate Constants. Measurements of the bimolecular rate constants for the addition of $^{\bullet}OH$ to $C_6H_5NO_2$ were conducted at 250 bar and temperatures from 22 to 390 °C. As mentioned above, the pressure of 250 bar was chosen to ensure that the bimolecular rate constants were measured at single phase conditions throughout the entire temperature range. This resulted in a density decrease of pure water from 0.9971 g cm^{-3} at 25 °C and 1 bar to 0.2157 g cm^{-3} at 390 °C and 250 bar. Mixture densities should be quite similar to these values since the highest nitrobenzene concentration used was just 14 mM at ambient conditions. At the reaction conditions the highest concentrations of nitrobenzene were even less since the solution density is lower at higher temperatures. Values of k_{bi} for the reaction of $^{\bullet}OH$ with $C_6H_5NO_2$ were obtained from the slopes of the k_{obs} versus $C_6H_5NO_2$ concentration curves, according to eq 8. Examples are shown in Figure 6 for three representative temperatures. As seen in Figure 6, for a given temperature and pressure multiple data were taken at each nitrobenzene concentration. All of these data were used to determine the k_{bi} values from the slopes of the quenching plots. The uncertainty in the experimental bimolecular rate constants was determined from the 95% confidence intervals on the slopes of the quenching plots. Thus, the uncertainty that we report results from the variability in the replicate experiments at a given concentration. The final results, the bimolecular rate constants, are shown in Figure 7, along with the uncertainty at each temperature indicated by error bars. It should be noted that at several temperatures (200, 275, and 390 °C), we ran complete replicate sets of experiments with entirely different solutions and on entirely different days. In fact, the time between some of these replicate experiments was greater than a year. As shown in Figure 7, the replicates are all entirely consistent within experimental uncertainty.

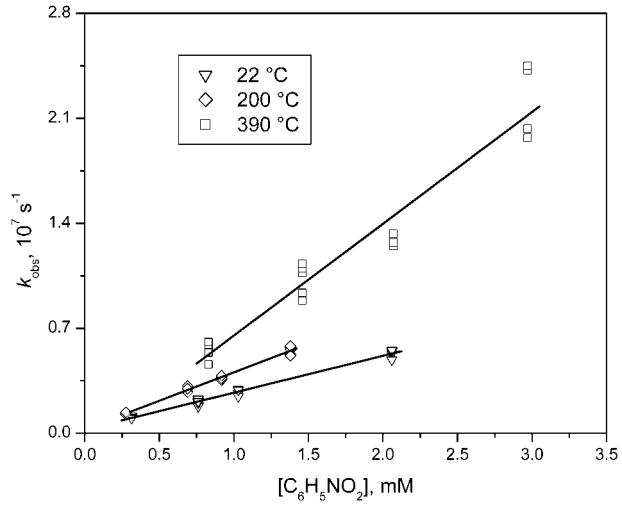

Figure 6. The effect of nitrobenzene concentration on the observed rate constant, k_{obs}, for the reaction between hydroxyl radical and nitrobenzene at 22, 200, and 390 °C.

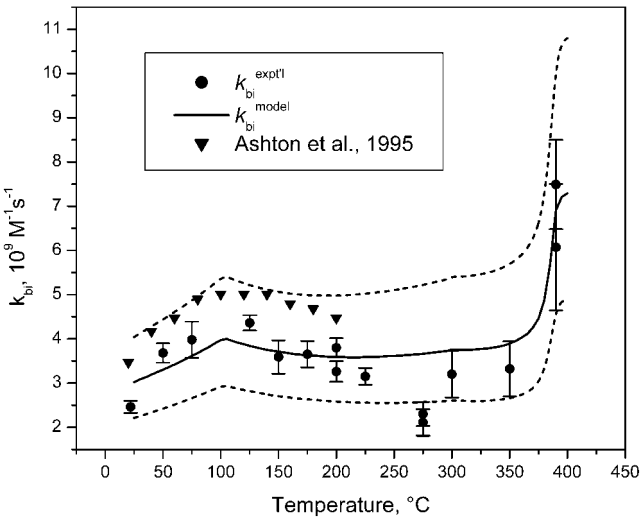

Figure 7. Comparison between the experimental and modeled bimolecular rate constants, k_{bi}, with 95% confidence intervals, for the reaction between hydroxyl radical and nitrobenzene at 250 bar and temperatures between 25 and 390 °C. The solid line is the model result using Arrhenius parameters fit to the experimental data between 25 and 225 °C. The line at $T > 225$ °C represents a prediction of the rate constants using Arrhenius parameters determined from the lower temperature data. The two dashed lines are the 95% confidence intervals on the predicted k_{bi} values. The data of Ashton et al.[1] are also included on the graph for comparison.

Discussion

The effect of temperature on our measured values of the bimolecular rate constants is shown in Figure 7. Also shown on this graph are the data of Ashton et al.,[1] as well as the kinetic model, which will be discussed below. As can be seen in the figure, the data obtained in this study match the Ashton et al.[1] data, which are available up to 200 °C, reasonably well. In addition, our value of the bimolecular rate constant, $(2.46 \pm 0.14) \times 10^9$ M^{-1} s^{-1}, at 22 °C and 250 bar, indicates that the pressure effect on the rate constant is not substantial since the literature value for the rate at ambient temperature and pressure is $(3.2 \pm 0.4) \times 10^9$ M^{-1} s^{-1}.[28] At 250 bar the bimolecular rate

(40) Bennett, G. E.; Johnston, K. P. *J. Phys. Chem.* **1994**, *98*, 441−447.
(41) Lee, D. S.; Park, S. D. *J. Hazard. Mater.* **1996**, *51*, 67−76.

Table 1. Nitrobenzene and Hydroxyl Radical Radii and Diffusion Coefficients

	$r_{\bullet OH}$, nm	$r_{C_6H_5NO_2}$, nm	$D_{\bullet OH}$, 10^{-5} cm^2 s^{-1}, 25 °C		$D_{C_6H_5NO_2}$, 10^{-5} cm^2 s^{-1}, 25 °C
			eq used	result at 25 °C	
Ashton et al.[1]	0.22	0.18	from ref 45	2.31	0.4
This work	0.22	0.55	Stokes−Einstein	1.73	0.92

constants increase slightly at temperatures up to about 125 °C. Although the rate constant is essentially at the diffusion-controlled limit at ambient conditions, even by 125 °C it has fallen well below diffusion control. The non-Arrhenius behavior of k_{bi} is evident, especially at temperatures between 125 and 350 °C, where the rate constants actually decrease slightly with increasing temperature. At temperatures above 350 °C, the qualitative behavior as a function of temperature changes, and k_{bi} increases rapidly with increasing temperature. This is apparent even though the uncertainty in the 390 °C measurements is greater than at lower temperatures due to the decreased signal-to-noise ratio at high-temperature conditions. To our knowledge, these are the first measurements of the rapid increase in the bimolecular rate constant at slightly subcritical and supercritical conditions for hydroxyl radical addition in water. It should be reiterated that the rate constants are well below the diffusion-controlled limit, except at ambient temperature.

Proposed Three-Step Reaction Mechanism (Ashton et al.[1]). In an effort to explain the insensitivity of the bimolecular rate constant for the addition of hydroxyl radical to nitrobenzene (as well as benzene, chlorobenzene, benzoate ion, and benzoic acid) at temperatures from ambient to 200 °C, Ashton et al.[1] proposed the formation of an intermediate π-complex. A variety of π and molecular complexes have been observed in numerous spectroscopic investigations.[42−44] Thus, the overall reaction of $^{\bullet}$OH with $C_6H_5NO_2$ to form a relatively stable σ addition complex shown in eq 9 may be composed of three steps (eqs 10−12).

$$^{\bullet}OH + C_6H_5NO_2 \xrightarrow{k_{bi}} [OHC_6H_5NO_2]_{\sigma}^{\bullet} \rightarrow \text{products} \quad (9)$$

$$^{\bullet}OH + C_6H_5NO_2 \xrightarrow{k_{10}} [OHC_6H_5NO_2]_{\pi}^{\bullet} \quad (10)$$

$$[OHC_6H_5NO_2]_{\pi}^{\bullet} \xrightarrow{k_{11}} {}^{\bullet}OH + C_6H_5NO_2 \quad (11)$$

$$[OHC_6H_5NO_2]_{\pi}^{\bullet} \xrightarrow{k_{12}} [OHC_6H_5NO_2]_{\sigma}^{\bullet} \quad (12)$$

According to this mechanism, reaction 9 occurs based on the formation of a π-intermediate (reaction 10), which can either dissociate back to the reactants (reaction 11) or lead to the formation of the observed σ-intermediate product (reaction 12). Ashton et al.[1] suggested that the formation of the π-intermediate, the result of the electrophilic $^{\bullet}$OH interacting with π-electrons of the aromatic ring, is the precursor of the more stable σ-complex.

If one applies steady-state analysis to [$^{\bullet}OHC_6H_5NO_2$], the k_{bi} of reaction 9 is given by:

$$k_{bi} = \frac{k_{10}k_{12}}{k_{11} + k_{12}} \quad (13)$$

In the proposed mechanism, Ashton et al.[1] assumed that reaction 10 was diffusion controlled but reactions 11 and 12 had activation barriers.

Table 2. Preexponential Factors and Activation Energies for Eqs 11 and 12

	A_{11}/A_{12}	$E_{11} - E_{12}$, kJ mol^{-1}
Ashton et al.[1]	1893.49[a]	18.7[a]
this work	1799.20 ± 455.89	15.09 ± 0.82

[a] Calculated from values of A_{11}, A_{12}, E_{11}, and E_{12} given by Ashton et al.[1]

The Smoluchowski equation was used by Ashton et al.[1] to calculate the diffusion-controlled rate constant of reaction 10, as shown in eq 14:

$$k_{10} = 4\pi(D_{\bullet OH} + D_{C_6H_5NO_2})(r_{\bullet OH} + r_{C_6H_5NO_2}) \quad (14)$$

This requires the diffusion coefficients and the molecular radii of the two reactants. Ashton et al.[1] used values for $D_{\bullet OH}$ and $r_{\bullet OH}$ from the literature,[45] where $r_{\bullet OH}$ is a constant but $D_{\bullet OH}$ increases with temperature, roughly according to the Stokes−Einstein equation (i.e., the diffusion coefficient is inversely proportional to the viscosity). $D_{C_6H_5NO_2}$ and $r_{C_6H_5NO_2}$ were obtained as the values that best fit the three-step model to the reaction kinetics data, as determined by simple inspection. Surprisingly, Ashton et al.[1] did not use the value of $r_{C_6H_5NO_2}$ that is also available in the literature.[45] The activation energies and preexponential factors for reactions 11 and 12 were fit to the experimental kinetics data. However, the activation energies and preexponential factors of the two reactions cannot be determined independently, as we will explain below. Thus, the values presented by Ashton et al.[1] are just one set of a family of an infinite number of sets that fit the experimental values equally well. The values of the reactant radii and diffusion coefficients at 25 °C used by the Ashton et al.[1] group are shown in Table 1 and the Arrhenius parameters they obtained are shown in Table 2.

Ashton et al.[1] found that this three-step model represented the experimental kinetics quite well, not just for the rates of the reaction of $^{\bullet}$OH with nitrobenzene, but for the reaction of $^{\bullet}$OH with benzene, chlorobenzene, benzoate ion, and benzoic acid, as well. The temperature dependence of k_{bi} is roughly the same for the reaction of $^{\bullet}$OH with each of these compounds, although the absolute values of k_{bi} do differ. Clearly, the substituents on the benzene ring have no effect on the temperature dependence of k_{bi}. Thus, we would expect the temperature dependence of the bimolecular rate constants of those compounds with $^{\bullet}$OH to be similar at slightly subcritical and supercritical temperatures to what we observe for the reaction of $^{\bullet}$OH with $C_6H_5NO_2$.

(42) Raner, K. D.; Lusztyk, J.; Ingold, K. U. *J. Phys. Chem.* **1989**, *93*, 564−570.
(43) Mulliken, P. S. *Molecular Complexes*; Wiley-Interscience: New York, 1969.
(44) Foster, R. *Organic Charge-Transfer Complexes*; Academic: New York, 1969.
(45) Elliot, A. J.; McCracken, D. R.; Buxton, G. V.; Wood, N. D. *J. Chem. Soc., Faraday Trans.* **1990**, *86*, 1539−1547.

Model Results (This Work). One of our objectives is to determine if the mechanism proposed by Ashton et al.[1] can model our new measurements of k_{bi} at high temperatures (from 200 to 390 °C, 250 bar), which showed strong temperature dependence, *using only parameters determined at lower temperatures*. Thus, we used the lower temperature experimental results obtained in this work (from ambient to 225 °C) and obtained apparent Arrhenius parameters (A_{11}/A_{12} and $E_{11} - E_{12}$) for reactions 11 and 12. These Arrhenius parameters were then used to predict the bimolecular rate constants at temperatures from 225 to 390 °C. The methods used to estimate the Arrhenius parameters and the diffusion coefficients will be described in the following paragraphs.

Like Ashton et al.,[1] we used the Smoluchowski equation to calculate the rate of the diffusion-controlled encounter between •OH and $C_6H_5NO_2$ (reaction 10). The main differences in the current work are the value of $r_{C_6H_5NO_2}$ and the methods used to estimate the diffusion coefficients. In the current study, we use values of both $r_{\bullet OH}$ and $r_{C_6H_5NO_2}$ taken from literature,[45] which show that the size of nitrobenzene is significantly larger than the size of the hydroxyl radical, as one would expect.

Recently, Butenhoff et al.[46] have shown that the Wilke−Chang equation (eq 15) provides a better estimation of diffusion coefficients in supercritical water than the Stokes−Einstein (S−E) equation. Therefore, we chose to use the Wilke−Chang equation to estimate the diffusion coefficient of $C_6H_5NO_2$ at all temperatures,

$$D_{C_6H_5NO_2} = 7.4 \times 10^{-8} \frac{(\phi M_{H_2O})^{0.5} T}{\eta_{H_2O} V_{C_6H_5NO_2}^{0.6}} \qquad (15)$$

where ϕ is the association factor of the solvent: 2.26 was used for water at temperatures from ambient to 384 °C,[47] 1.0 was used at temperatures of 385 °C and above[47] because SCW resembles a nonaqueous and unassociated solvent and the dielectric constant is only 5.7 at the critical point. $V_{C_6H_5NO_2}$ is the molar volume of $C_6H_5NO_2$ at its normal boiling temperature and this value was estimated using a standard correlation,[47] resulting in a value of 123.7 $cm^3\ mol^{-1}$.

Since the molar volume, V_{OH}, of •OH at its normal boiling point is not available, we were forced to use the simpler Stokes−Einstein (S−E) model, eq 16, to calculate the diffusion coefficient of •OH. In the S−E equation the diffusion coefficient is inversely proportional to the viscosity, which can be taken from the literature.[36]

$$D_{\bullet OH} = \frac{RT}{4\pi\eta r_{\bullet OH}} \qquad (16)$$

This yields a diffusion coefficient of hydroxyl radical at ambient conditions that is reasonable. However, it is 30% less than that used by Ashton et al.[1] and 30% less than the self-diffusivity of water at ambient conditions which is $2.3 \times 10^9\ m^2\ s^{-1}$.[48] The parameters used in the Smoluchowski equation in the current work are compared with the ones used by Ashton et al.[1] in Table 1. Both sets of parameters (in conjunction with the Arrhenius parameters discussed below) give good representations of the lower temperature data.

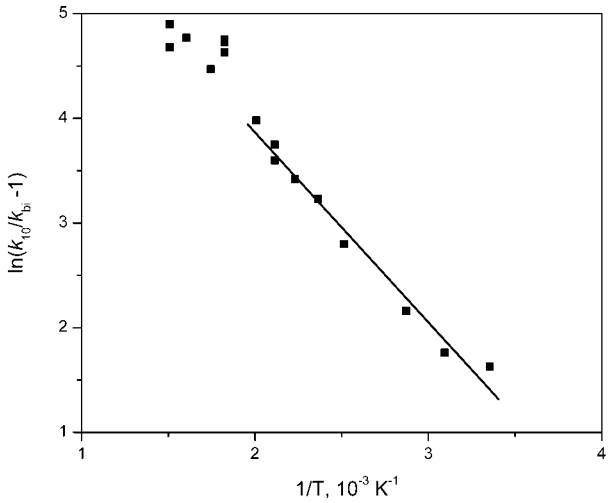

Figure 8. Arrhenius plot of eq 18 for the experimental values from ambient to 390 °C. The solid line is the linear regression fit using experimental values from ambient to 225 °C.

Equation 13 can be rewritten by dividing by k_{10}, the diffusion contribution to the bimolecular rate constant, to obtain

$$\frac{k_{bi}}{k_{10}} = \frac{k_{12}}{k_{11} + k_{12}} \qquad (17)$$

The rate constants for the kinetically controlled reactions (eqs 11 and 12) can be expressed as $A_{ij}\exp(-E_{ij}/RT)$, where A_{ij} is the preexponential factor, E_{ij}, is the activation energy, R is the gas constant, and T is the temperature. If we invert eq 17, use the Arrhenius parameters, A_{11}, A_{12}, E_{11}, and E_{12}, to represent k_{11} and k_{12}, and take the natural logarithm, it is clear that the model is linear with respect to $1/T$, as shown in eq 18 below.

$$\ln\left(\frac{k_{10}}{k_{bi}} - 1\right) = \ln\left(\frac{A_{11}}{A_{12}}\right) - \frac{(E_{11} - E_{12})}{R}\frac{1}{T} \qquad (18)$$

It is also clear from eq 18 why the Arrhenius parameters for the two kinetically controlled reactions cannot be determined independently. They only appear as a preexponential factor ratio and an activation energy difference. We will refer to these combined parameters as the *apparent* preexponential factor (A_{11}/A_{12}) and *apparent* activation energy ($E_{11} - E_{12}$). It is for this reason that we only show A_{11}/A_{12} and $E_{11} - E_{12}$ used by Ashton et al.[1] in Table 2, even though they reported individual values of the Arrhenius parameters.

The experimental data for the bimolecular rate constants divided by the calculated diffusion-controlled rate constants (k_{10}; see modeling method described above) were plotted as suggested by eq 18 and this is shown in Figure 8. The low-temperature data (up to 225 °C) were regressed with a linear fit to minimize the sum of the squares of the deviation between the data and the predicted values using ORIGIN software (version 6, Microcal Software Inc.). As indicated by eq 18, the apparent preexponential factor (A_{11}/A_{12}) and the apparent activation energy ($E_{11} - E_{12}$) were obtained from the intercept and slope of the plot. In addition, the 95% confidence intervals on these

(46) Butenhoff, T. J.; Goemans, M. G. E.; Buelow, S. J. *J. Phys. Chem.* **1996**, *100*, 5982−5992.
(47) Green, D. W. *Perry's Chemical Engineering Handbook*, 6th ed.; McGraw-Hill Book Company: New York, 1984.
(48) Mills, R. *J. Phys. Chem.* **1973**, *77*, 685−688.

parameters were computed and the values of the apparent Arrhenius parameters with uncertainties are reported in Table 2.

The predicted bimolecular rate constant, k_{bi}, from ambient to 400 °C was then calculated according to eq 18 using the apparent Arrhenius parameters determined only from the lower temperature (ambient to 225 °C) data. These values are shown as the solid line in Figure 7. The model accurately predicts the relative insensitivity of the bimolecular rate constant to temperature in the region up through 350 °C. More interestingly, it also predicts the increase in k_{bi} at temperatures above 350 °C, as is observed experimentally. The 95% confidence intervals on the predicted k_{bi} values were also obtained from the linear regression of the low-temperature data using eq 18. These confidence intervals are shown as the dashed lines in Figure 7.

It should be reiterated that only the experimental data between ambient and 225 °C, which show very little temperature dependence, were used to estimate the apparent Arrhenius parameters. From Figure 7 it is clear that both our data and those of Ashton et al.[1] fall within the upper and lower 95% confidence intervals of the model results at temperatures from ambient to 225 °C. Clearly, the proposed mechanism captures the small temperature effect on k_{bi} in the region up to 225 °C remarkably well.

More importantly, we are interested in whether this model can explain the temperature effect on the experimental values of k_{bi} at temperatures above 225 °C, i.e., at slightly subcritical and supercritical conditions. The rate constants, k_{bi}, were estimated according to eq 18 at temperatures above 225 °C using the apparent Arrhenius parameters given in Table 2 that were fit to the lower temperature data. The diffusion coefficients for the reacting species at these temperatures were estimated using eqs 15 and 16. The predicted values match the experimental data within the 95% confidence intervals for all temperatures except 275 °C, where the model does not adequately capture the minimum in the rate constant. Nonetheless, the model does predict an increase in the bimolecular rate constants at higher temperatures, as shown in Figure 7. The major factor in determining the magnitude of the rate constant increase at high temperatures is the diffusion coefficients of the species that determine k_{10}. According to the model, the large increase in k_{bi} in the slightly subcritical and supercritical regions is due entirely to the dramatic decrease in water density and viscosity, and subsequent increase in diffusion coefficients, that occurs near the critical point.

Thus, we conclude that the three-step mechanism suggested by Ashton et al.,[1] based on measurements to just 225 °C, is able to model the bimolecular rate constants for the addition of $^{\bullet}OH$ to $C_6H_5NO_2$ at conditions through the supercritical region. Since Ashton et al.[1] showed that the addition of $^{\bullet}OH$ to benzene, chlorobenzene, benzoate ion, and benzoic acid showed similar non-Arrhenius behavior at temperatures below 200 °C, it is entirely possible that the temperature effect at subcritical and supercritical conditions on the rates of those reactions would be similar to that shown in Figure 7.

Summary

We report the bimolecular rate constants for the addition reaction of $^{\bullet}OH$ to $C_6H_5NO_2$ in water at temperatures between ambient and 390 °C and at a pressure of 250 bar. $^{\bullet}OH$ was generated using pulse radiolysis and the kinetics determined by monitoring the growth of the nitrohydroxycyclohexadienyl radical. These are among the first direct measurements of hydroxyl radical reactivity in supercritical water. Hydroxyl radical is one of several important oxidizing species in supercritical water oxidation and this work is a first step toward the measurement of rates of hydrogen abstraction by hydroxyl radical in supercritical water.

The measured bimolecular rate constants showed non-Arrhenius temperature dependence from ambient to 350 °C, but increase significantly at slightly subcritical and supercritical conditions. A three-step reaction mechanism including the formation of a π-complex intermediate as the precursor of the nitrohydroxycyclohexadienyl radical, proposed by Ashton et al.,[1] was introduced to model the experimental results. This mechanism, using parameters determined from the lower temperature measurements (below 225 °C), is able to model the bimolecular rate constants for the addition of $^{\bullet}OH$ to $C_6H_5NO_2$ at conditions through the supercritical region if accurate values of the species diffusion coefficients are available. However, the calculated k_{bi} depend heavily on the model chosen to estimate the diffusion coefficients of the hydroxyl radical.

Acknowledgment. This research has been supported by the U.S. Army Research Office (Grant no. DAAG55-97-1-0025) and National Science Foundation (Grant no. EEC97-00537-CRCD). We wish to thank the Notre Dame Radiation Laboratory, which is supported by the Office of Basic Energy Sciences of the U.S. Department of Energy, for use of their facilities. We also wish to thank the personnel at this Laboratory for their help and suggestions.

JA0110980